Sensors and Materials, Vol. 34, No. 9 (2022) 3593–3605
MYU Tokyo

S & M 3063

Single-layer, Slot-loaded, Substrate-integrated Waveguide Cavity-backed Circular Polarization Filtering Antenna

Jia-Xiang Chen,[1] Hai-Tao Xing,[1*] You-Yi Ke,[2] Chen Li,[1] and Zhong-Hua Ma[1]

[1]School of Marine Information Engineering, Jimei University, Xiamen, Fujian 361021, China
[2]Ruijie Networks Co., Ltd., Fuzhou, Fujian 350008, China

(Received April 21 2022; accepted September 12, 2022)

Keywords: axial ratio, bandpass filter (BPF), circular polarization (CP), substrate-integrated waveguide (SIW)

A low-profile slot-loaded circular polarization (CP) filtering antenna of a substrate-integrated waveguide (SIW) is proposed in this paper. It is composed of a bandpass filter with an SIW inversely coupled resonant structure, an SIW cavity feeding structure, and a surface-loaded rectangular slot SIW radiation cavity. Two L-type SIW cavity resonators surrounding the radiation cavity excite the rectangular slot through openings in the sidewalls formed by metallic vias. The bandpass filter consists of three SIW rectangular cavities in parallel. The size of the cavity and the width of the coupling port are changed to adjust the bandpass characteristics. Four rectangular slots loaded by an SIW radiation cavity are used to form a rectangular ring structure. The four rectangular slots are excited by excitation signals with phases of 0, 90, 180, and −90°. The electromagnetic wave radiated by these slots is synthesized into a circularly polarized wave in the far field. For demonstration, the prototype antenna is designed, manufactured, and measured. The center frequency of the filtering antenna is 28 GHz, the impedance broadband width is about 456 MHz (1.6%), and the gain in the working band is 4.16–5.23 dBi. The axial ratio bandwidth is 270 MHz (0.9%). The measured results are consistent with the simulation results. Owing to its good performance, the proposed filtering antenna is expected to be widely used as a novel RF sensor in various IoT devices.

1. Introduction

To miniaturize devices and improve the efficiency of the system in the rapid development of wireless communication systems, it is necessary to integrate multiple microwave/RF devices.(1) As an RF sensor, the antenna obtains information by sensing electromagnetic waves in space. The electromagnetic environment in space is very complex and affects the reliability of the signal received by a traditional antenna. Integrating the antenna with a filter will effectively solve this problem. The antenna and filter are the two necessary and most important components in the front-end parts of RF systems for wireless communication. The antenna receives and transmits signals, and the filter selects useful signals and suppresses out-of-band interference

*Corresponding author: e-mail: xht2005@jmu.edu.cn
https://doi.org/10.18494/SAM4019

ISSN 0914-4935

signals.[2,3] To improve the system performance and miniaturize the RF front-end, the concept of a filtering antenna was proposed. A filtering antenna is realized by integrating the antenna and filter by embedding the filter circuit into the feed network of the antenna. Filtering antennas have excellent performance characteristics, reducing the volume of equipment, improving the transmission efficiency, eliminating interference and noise, and maintaining the filtering function and radiation characteristics of the antenna.[4,5] Researchers have proposed various effective methods for realizing a filtering antenna, and they have striven to integrate the filter and antenna, such as by directly combining them,[6] by adding the filter circuit to the antenna feed network,[7] by etching an e-slot on the radiator, and by loading the short-circuit pin.[8]

Nadan *et al.* proposed the first prototype of an integrated filter and antenna.[9] This filtering antenna has a multilayer coplanar structure to integrate a Chebyshev filter and a dipole antenna, and it has good broadband matching and radiation characteristics. Wu *et al.* developed an integrated filtering antenna composed of a microstrip square ring with two openings, a coupling line, and a Γ integrated microstrip filter.[10] The Γ-shaped microstrip antenna is not only a radiator, but also a resonator of the bandpass filter. It mainly works at 2.45 GHz, and the transmission loss between the filter and the antenna is close to zero. Wang *et al.* reported an integrated planar filtering antenna composed of a second-order band-stop filter unit with an absorption branch line and a planar quasi-Yagi antenna in parallel.[11] The out-of-band radiation is effectively suppressed, and the inner-band gain ripple is less than 1 dB.

A substrate-integrated waveguide (SIW) has advantages of low profile, light weight, low cost, low loss, and easy-to-build circuit boards. It is widely used to design millimeter wave filters and SIW slot antennas. Yusuf *et al.* proposed an integrated 3D vertical cavity filter based on an SIW and slot antenna.[12] The relative bandwidth reached 3% at the center frequency of 10.16 GHz, and the transition loss was small. They vertically integrated three SIW cavity filters and antennas in an array, achieving a transition loss close to zero, improving the efficiency of the filtering antenna, and reducing the occupied space, but there were large side lobes on the E-plane.[13] Liu *et al.* proposed a hybrid antenna with a single-layer SIW cavity and a circular patch resonator that had a wide band and excellent selectivity.[14] The antenna consisted of a circular patch resonator, a square SIW cavity, and nine metal pins. The metal pins were used to enhance the frequency selectivity of the low stopband. The working frequency band ranged from 3.27 to 3.74 GHz. There were two out-of-band radiation zeros, and the gain reached 7.3 dBi. Although the above integrated filtering antennas had a small device volume and superior frequency band selectivity, most filtering antennas are limited to linear polarization, which makes them unsuitable for some emerging applications.

To reduce polarization loss and suppress multipath loss, it is necessary to study the circular polarization (CP) characteristics of filtering antennas. Because the design parameters of circularly polarized filtering antennas are very sensitive, their design is challenging. Hua *et al.* proposed a SIW circularly polarized filtering antenna based on a dual-mode cavity.[15] The filtering characteristics were realized by the coupling resonant circuit of two dual-mode SIW cavities in the same plane, and the circularly polarized radiation was realized by a non-uniform annular slot integrated with the back cavity. Li and Gong integrated two high-Q SIW cavity filters with a CP patch antenna through a coupling slot to achieve a third-order filter response.[16]

The axial ratio (AR) bandwidth of a single antenna element is narrow, and complex feed network and array structures are required to improve the bandwidth. Ji *et al*. proposed a single-feed, low-profile, circularly polarized antenna with a bandpass filter response.[17] Their antenna used the leakage field of the SIW edge via to excite four orthogonal half-mode radiation patches to realize circularly polarized radiation based on the planar SIW dual-mode (TE_{102}/TE_{201}) cavity, but the structure was complex, the AR bandwidth was narrow, and the efficiency was low. Jung *et al*. adopted an SIW rear cavity annular slot antenna and coaxial feed to reduce connection loss and enhance broadband impedance-matching characteristics.[18] Their array antenna required a complex feeding structure. Although the antenna had advantages of low profile, low loss, and low cost, its impedance and AR bandwidths were very narrow and it had no filtering characteristics. Starting from the working principle of a dual-mode SIW cavity circularly polarized antenna, Zhan and Dong added a slot in the top layer of an SIW cavity and obtained circularly polarized radiation characteristics based on orthogonal mode current.[19] However, the filtering characteristics of the integrated antennas in Refs. 18 and 19 were poor. Thus far, there has been little research on SIW circularly polarized filtering antennas.

In this paper, we propose an SIW circularly polarized filtering antenna with a bandpass filter response at a frequency of 28 GHz. The filter part is an inverse coupling resonator based on the SIW structure. The circularly polarized antenna and filter are in the same plane. Two L-shaped SIW cavities surrounding the SIW radiation cavity induce orthogonal excitation to the four rectangular slots of the SIW radiation cavity, synthesizing circularly polarized radiation characteristics in the far field. The proposed antenna has good CP bandpass filtering characteristics, a compact structure, and a low profile. It can be used as an electromagnetic sensor in various communication devices.

2. Design of Filtering Antenna Structure

Figure 1 shows the geometric structure of the designed SIW-based CP filtering antenna, which is manufactured on a single-layer Rogers RT/Duroid 5880 substrate with a thickness of 0.7874 mm, a permittivity of 2.2, and a loss tangent of 0.0009. The bandpass filter is composed of three SIW cavities side by side. The size of the different SIW cavities and the width of the cavity coupling port are changed to adjust the bandpass characteristics. The four via walls of the middle SIW radiation cavity are opened with feed excitation ports of different sizes, and excitation signals of different phases and amplitudes are input from the peripheral SIW cavity. Four rectangular slots facing the opening are loaded on the top of the SIW radiation cavity to induce slot radiation, resulting in the synthesis of circularly polarized radiation waves in the far field.

The three side-by-side SIW cavities constituting the filter are directly excited by a microstrip feeder with a characteristic impedance of 50 Ω. The size of the SIW cavity is related to the corresponding resonance frequency[20] as follows:

$$f = \frac{c}{2\pi\sqrt{\mu_r \varepsilon_r}} \sqrt{\left(\frac{\pi}{W_{eff}}\right)^2 + \left(\frac{\pi}{l_{eff}}\right)^2}. \quad (1)$$

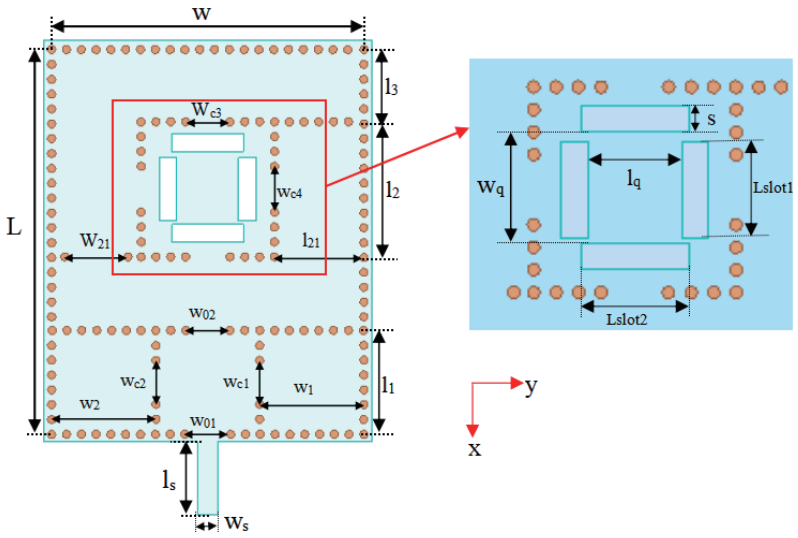

Fig. 1. (Color online) Structure of proposed CP filtering antenna.

In the TE_{10} dominant mode, W_{eff} and l_{eff} are the equivalent width and length of the SIW cavity, which are expressed as

$$W_{eff} = w - \frac{\phi^2}{0.95d}, \tag{2}$$

$$l_{eff} = l - \frac{\phi^2}{0.95d}, \tag{3}$$

where w and l are the true width and length of the SIW cavity, respectively, ϕ is the diameter of the metallic cylinder, and d is the distance between adjacent metallic cylinders. The parameters of the metallic cylinder are one of the most important aspects of the SIW model design. The design parameters of the metallic cylinder are[21]

$$\phi < \frac{\lambda_g}{5}, \tag{4}$$

$$d \le 2\phi. \tag{5}$$

The SIW cavity forms an inverse coupling resonator with filtering characteristics. The variation in SIW cavity size leads to a change in resonant frequency. Coupling with the best matching is obtained by adjusting the opening width of the SIW cavity. Two L-shaped SIW cavities form a feed excitation part, which surrounds the SIW radiation cavity etched with four rectangular slots. The four rectangular slots loaded on the SIW radiation cavity are placed to surround a rectangular area (Fig. 1), and each slot is orthogonal to the input direction of the excitation signal. The signal after frequency selection by the bandpass filter is then fed by two

L-shaped SIW cavities to form excitation signals of 0, 90, 180, and −90° at the four openings of the via wall of the SIW slot radiation cavity. The excitation signals are finally radiated into space through the four rectangular slots and synthesized into circularly polarized waves in the far field.

Table 1 shows the parameters of the structure in Fig. 1 after optimization and adjustment. The size of the filtering antenna is $W \times L$ = 24.4 mm × 29.7 mm, the width of the radiation gap is 1.3 mm, and the other structural parameters are shown in Table 1.

3. Performance Analysis of CP Filtering Antenna

Figure 2 shows the curve variations of the impedance and 3 dB AR bandwidths when the rightmost cavity width W_1 of the SIW filter is reduced from 7.95 to 7.65 mm. As W_1 changes, the width of the cavity in the middle also changes accordingly. Figure 2(a) shows that when W_1 = 7.75 mm, the reflection coefficient in the band is optimal, the filtering characteristic is the best, and the impedance bandwidth reaches a maximum of 425 MHz. When W_1 increases or decreases from this value, parasitic resonance occurs near 29.5 GHz and the impedance bandwidth decreases slightly. Figure 2(b) shows that when W_1 varies, the AR bandwidth is almost unchanged. Hereafter, we select the optimal width W_1 = 7.75 mm to achieve the good impedance matching of the antenna and adapt to the ideal impedance and 3 dB AR bandwidths.

Table 1
Structural parameters of filtering antenna (unit: mm).

Ws	W_{01}	W_{02}	W_1	W_2	l_s	d	ϕ	W	l_q	W_q	W_{21}
2.15	3.4	3.3	7.7	7.75	5.4	1.1	0.6	24.4	4.6	5.4	4.7
s	W_{c1}	W_{c2}	W_{c3}	W_{c4}	l_1	l_2	l_3	L	L_{slot1}	L_{slot2}	l_{21}
1.3	3.24	3.25	3.3	3.4	7.7	10	5.35	29.7	4.7	5.3	6.65

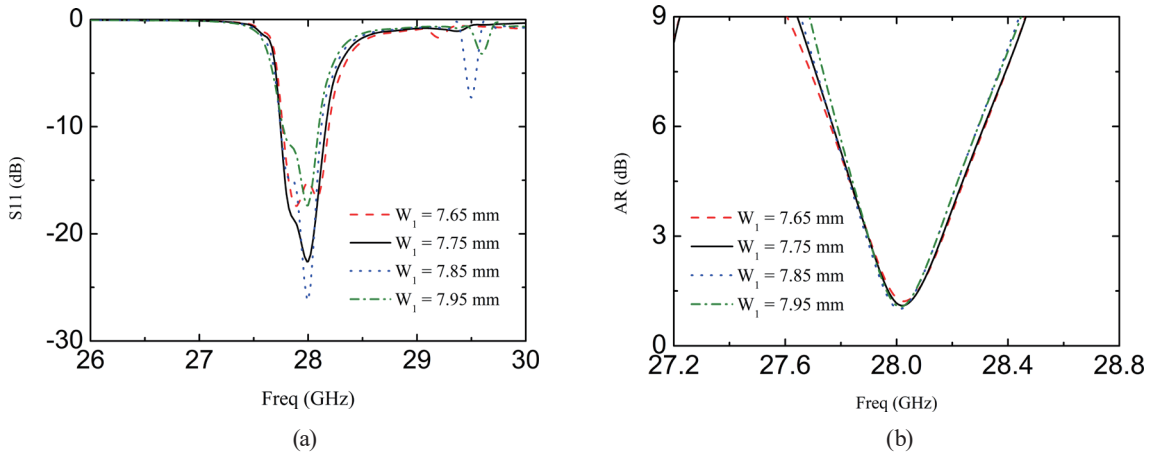

Fig. 2. (Color online) Simulation results for reflection coefficient and AR for different W_1 values: (a) reflection coefficient and (b) axial ratio.

Figure 3 shows the current distributions of the proposed filtering antenna at $t = 0$ and $t = T/4$. When $t = 0$, the current flows along the horizontal direction and mainly concentrates near the horizontal rectangular slot. When $t = T/4$, the current flows along the vertical direction and mainly concentrates near the vertical rectangular slot. In this way, the synthetic fields radiated by the orthogonal current are formed in the far field to implement the CP characteristic. Figure 4 shows the simulation results for the reflection coefficient and AR of the antenna when the length L_{slot1} of the two rectangular slots in the horizontal direction is changed. As shown in Fig. 4(a), when $L_{slot1} = 4.7$ mm, the antenna exhibits good reflection coefficient and in-band characteristics. Changing L_{slot1} has little effect on the reflection coefficient. Figure 4(b) shows that changing L_{slot1} has a major impact on the AR. When $L_{slot1} = 4.7$ mm, the center frequency is close to 28

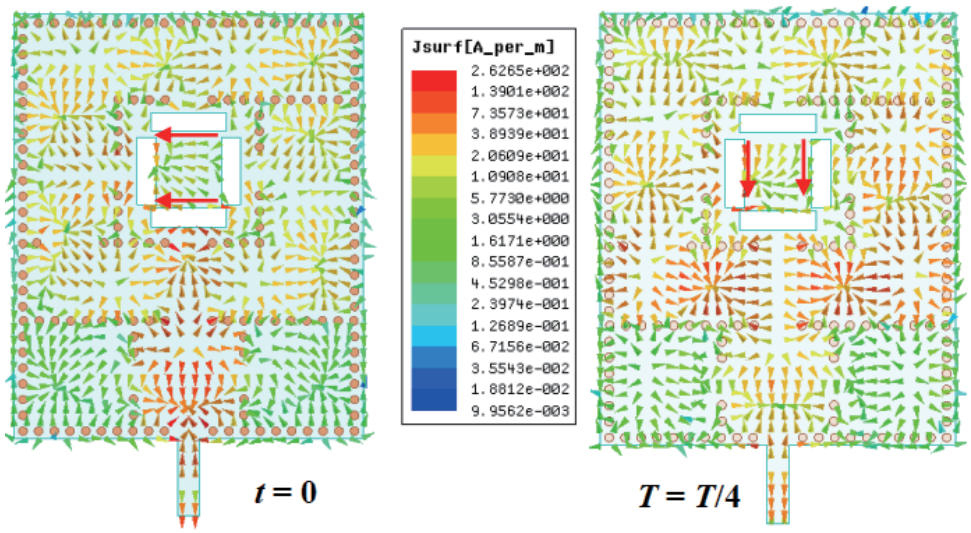

Fig. 3. (Color online) Current distributions of proposed filtering antenna at time periods of $t = 0$ and $t = T/4$.

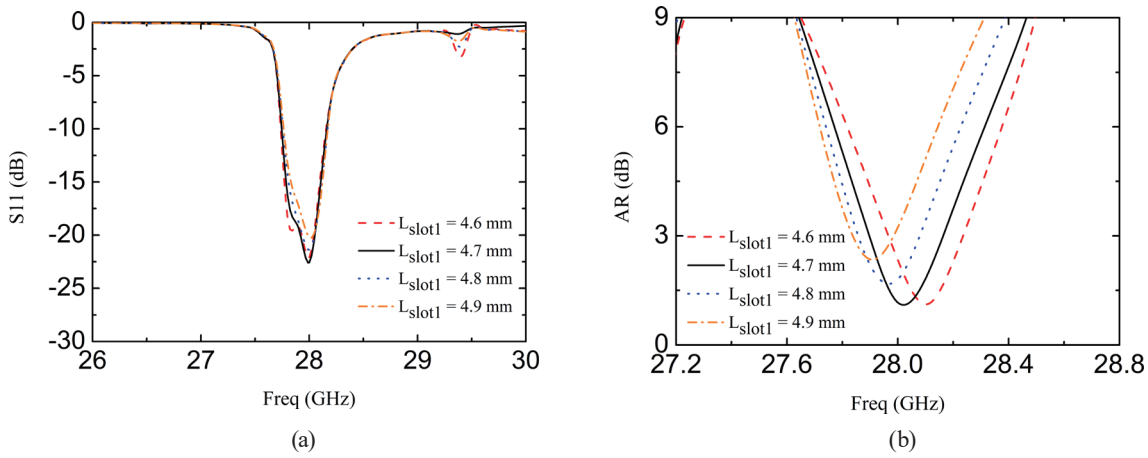

Fig. 4. (Color online) Simulation results for reflection coefficient and AR with different L_{slot1} values: (a) reflection coefficient and (b) axial ratio.

GHz, the 3 dB AR bandwidth is 270 MHz, and the AR is small. When L_{slot1} is decreased from 4.7 mm, the 3 dB AR band moves to a high frequency. When L_{slot1} is increased from 4.7 mm, the 3 dB AR band moves to a low frequency. Simultaneously, the AR bandwidth decreases rapidly and the AR increases. The distance between two rectangular slots in the horizontal direction will also have a major impact on the AR characteristics of the antenna. Figure 5 shows the simulation results for the AR when L_{slot1} is fixed at 4.7 mm and the distance l_q between the two rectangular slots is gradually increased from 4.4 to 5 mm in steps of 0.2 mm. When l_q is greater than 4.6 mm, the AR characteristics deteriorate and the working frequency band shifts to a high frequency at the same time. When l_q is less than 4.6 mm, the AR increases slightly, the 3 dB AR bandwidth decreases, and the frequency band shifts to a low frequency. When l_q = 4.6 mm, the 3 dB AR bandwidth is the widest and the AR of the center frequency is the smallest.

Similarly, the rectangular slot in the vertical direction will also affect the AR characteristics of the antenna. Figure 6(a) shows the AR characteristics when the distance w_q between two

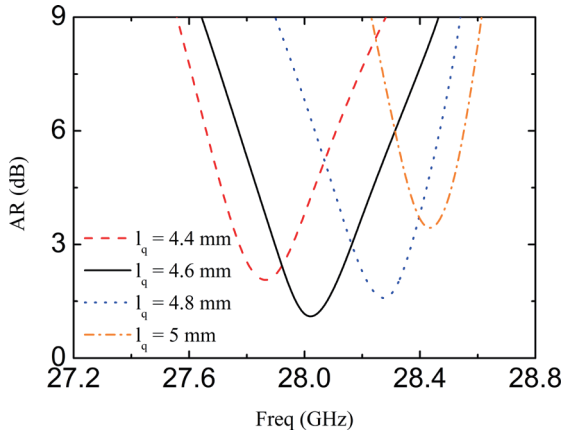

Fig. 5. (Color online) Simulation results for AR with different l_q values.

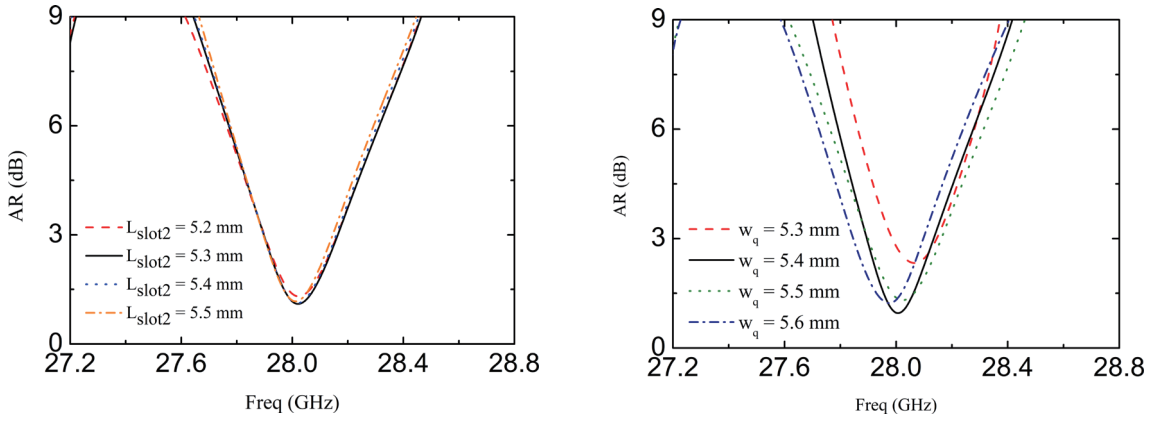

Fig. 6. (Color online) Simulation results of antenna AR with different L_{slot2} and W_q values: (a) length L_{slot2} of horizontal rectangular slots and (b) spacing W_q between horizontal rectangular slots.

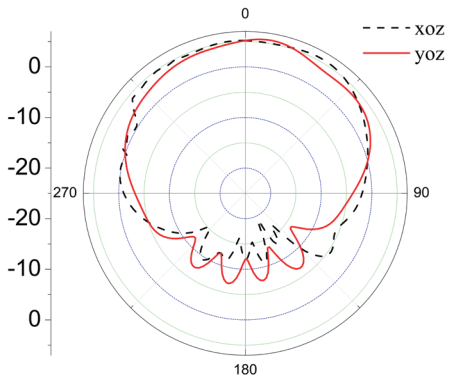

Fig. 7. (Color online) Simulated xoz and yoz plane radiation patterns at center frequency of 28 GHz.

horizontal rectangular slots in the vertical direction and the length L_{slot2} of the slot are changed. When the rectangular slot length L_{slot2} is varied from 5.2 to 5.5 mm in steps of 0.1 mm, there are no obvious changes in the AR characteristics of the antenna. Figure 6(b) shows the AR curves of the antenna when L_{slot2} is fixed at 5.3 mm and the distance w_q between two horizontal rectangular slots is changed. When w_q = 5.4 mm, the AR is the smallest and the bandwidth is the widest. When w_q deviates from 5.4 mm, the AR and 3 dB AR bandwidth both deteriorate. Therefore, for two rectangular slots in the vertical direction, the distance between them can be adjusted to improve the AR bandwidth. Figure 7 shows the radiation characteristics of the filtering antenna when the center frequency is 28 GHz. The radiation characteristics in the xoz and yoz planes are close to those in the half-space.

4. Measurement Results

An integrated CP filtering antenna with a bandpass response is fabricated and measured on a Rogers 5880 microwave substrate. A photograph of the antenna is shown in Fig. 8. To verify the simulation results, the filtering antenna is placed in an anechoic chamber and tested with a Ceyear 3672d vector network analyzer.

Figure 9 shows the simulated and measured reflection coefficients and gains of the filtering antenna. The measured center frequency of the CP filtering antenna is 28.01 GHz, which is very close to the simulation result of 28 GHz. The frequency band with a reflection coefficient smaller than −10 dB is from 27.72 to 28.176 GHz with a bandwidth of 456 MHz (1.6% FBW). The small difference between the measured and simulated impedance bandwidths can be attributed to the effects of the feeding SMA connector and manufacturing accuracy, as well as the possible deviation of the dielectric loss of the substrate. The measurement results in the passband are basically consistent with the simulation results. The measured peak gain of the filtering antenna varies in the range of 5.02 to 5.23 dBi with relatively smooth variation, which is slightly lower than that in the simulation. Figure 10 shows the measured AR curve of the filtering antenna. The AR bandwidth is 270 MHz (0.9% FBW) for an AR of less than 3 dB, which is

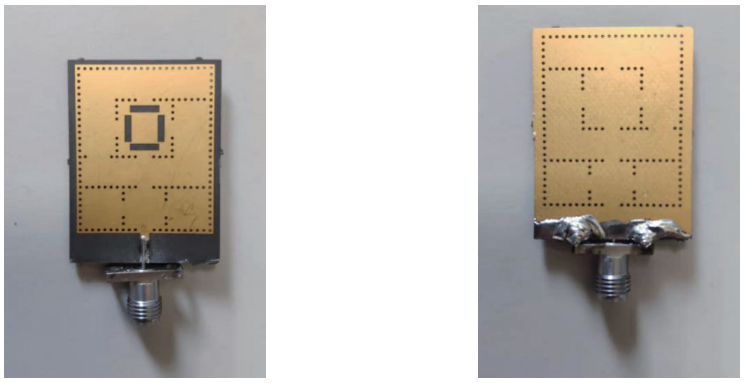

(a) (b)

Fig. 8. (Color online) Photograph of fabricated filtering antenna: (a) top and (b) bottom.

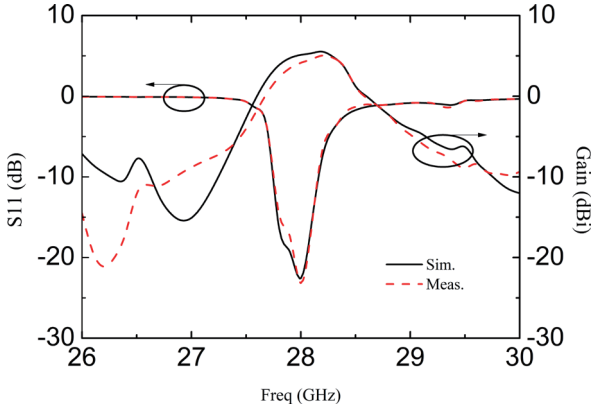

Fig. 9. (Color online) Simulated and measured reflection coefficients and gains.

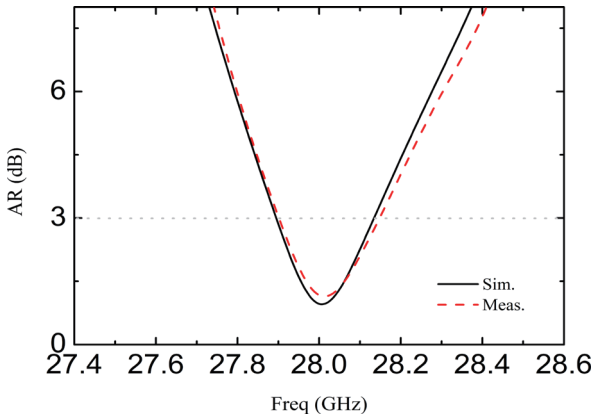

Fig. 10. (Color online) Simulated and measured AR characteristics.

consistent with the simulation result. Figure 11 shows the measured xoz and yoz plane radiation patterns of the CP filtering antenna when the working frequencies are 27.89, 28, and 28.16 GHz. A half-space radiation pattern is formed for each frequency, and the back lobe radiation is small because a ground plate is on the back side of the SIW.

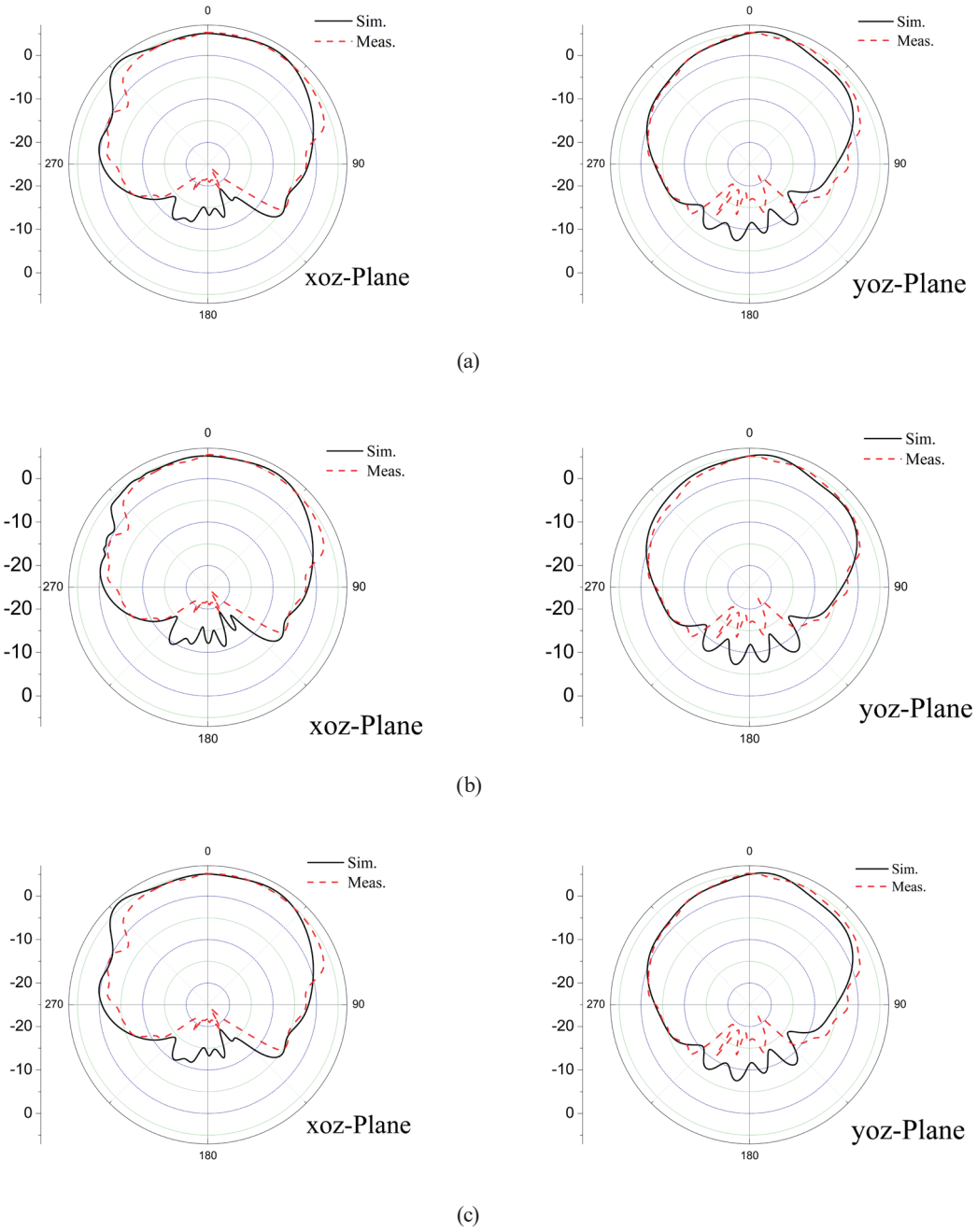

Fig. 11. (Color online) Measured radiation patterns of CP filtering antenna on xoz and yoz planes: (a) 27.89, (b) 28, and (c) 28.16 GHz.

In contrast with existing filter antennas, the filtering antenna based on the SIW structure in this paper adopted slot excitation CP characteristics, which enable the antenna to easily conform with the printed circuit board (PCB) and have a lower profile, good directionality, and a small area. Table 2 shows a comparison of the key results for the proposed filtering antenna and other CP filtering antennas. Referring to Table 2, the SIW-based filtering antennas proposed in Refs.

Table 2
Performance comparison of various filtering antennas.

Ref.	Center frequency (GHz)	Polarization	IBW (S11 < −10 dB) (GHz)	3 dB ARBW (GHz)	Antenna size (λ_0^3)	Gain (dBi)	Number of substrate layers	Structure type
5	37	LP	36.8–37.33	–	1.6 × 1.6 × 0.1	10.8	Multilayered	SIW
8	9.85	LP	9.76–9.932	–	0.86 × 1.16 × 0.1	6.1	1	SIW
12	10.16	LP	9.91–10.21	–	0.1 × 0.68 × 0.5	4.9	2	SIW
16	10.19	CP	9.85–10.55	9.9–10.03	0.56 × 0.44 × 0.13	6.77	2	SIW
17	5.03	CP	4.85–5.21	4.935–5.13	1.01 × 1.10 × 0.036	8	2	SIW
19	10.15	CP	10.1–10.35	10.11–10.19	1.58 × 0.92 × 0.03	9.4	1	SIW
22	4	CP	3.75–4.45	3.84–4.13	1.07 × 1.07 × 0.028	5.8	2	Microstrip patch
This paper	28	CP	27.72–28.17	27.89–28.16	2.28 × 2.7 × 0.07	5.23	1	SIW

IBW = impedance bandwidth, ARBW = axial ratio bandwidth.

5, 8, and 12 do not have CP characteristics. In contrast, the proposed design realizes not only the widest 3 dB AR bandwidth, but also good bandpass filtering response. The antenna proposed in Ref. 12 is composed of a two-layer PCB, whereas the antenna proposed in this paper is made of a single-layer PCB. This antenna has the characteristics of miniaturization and low profile. Although the antenna in Ref. 17 has a wide impedance bandwidth, the overlapping bandwidths (−10 dB impedance and 3 dB AR bandwidths) are much narrower than those for the newly proposed antenna. Zhan and Dong proposed several CP antennas based on a TE_{102}/TE_{201} mode SIW cavity, which have a high gain, but their AR bandwidth is only 80 MHz.[19] Although the 3 dB AR bandwidth of the filtering antenna proposed in Ref. 22 is slightly larger than that of the proposed design, its feed network is complex and is composed of a two-layer substrate, increasing the amount of occupied space.

5. Conclusions

On the basis of RF sensing technology, a single-layer slot-loaded SIW cavity-backed CP antenna with a bandpass filter response is designed, manufactured, and verified by experiments. The antenna is based on SIW technology and manufactured by a PCB process. The principles of CP radiation and bandpass filter response are analyzed and verified. The parameter design and processing technology of the antenna are analyzed in detail. The antenna achieves good bandpass filter response performance. The measured impedance bandwidth is 27.72–28.176 GHz (1.6%), the measured 3 dB AR bandwidth is 27.89–28.16 GHz (0.9%), and the measured peak gain is 5.23 dBi. The antenna has good radiation characteristics in space. In the future, the broadbandization, miniaturization, and functionalization of the filtering antenna can be realized by adopting new substrate materials, optimizing the SIW structure, and changing the feeding structure.

Acknowledgments

This work was supported by Fujian Natural Science Foundation Project (2022J01823).

References

1 D. M. Pozar: Microwave and RF Designs for Wireless Systems (John Wiley & Sons, 2000) 2nd ed., Chap. 2.
2 R. J. Cameron, C. M. Kudsia, and R. R. Mansour: Microwave Filters for Communication Systems: Fundamentals, Design, and Applications (John Wiley & Sons, 2007) 2nd ed., Chap. 3.
3 J. S. Hong: Microstrip Filter for RF/Microwave Applications (John Wiley & Sons, 2011) 2nd ed., Chap. 1.
4 Y. Zhang, X. Y. Zhang, L. H. Ye, and Y. M. Pan: IEEE Trans. Antennas Propag. **64** (2016) 3423. https://doi.org/10.1109/TAP.2016.2574872
5 H. Chu and Y. X. Guo: IEEE Trans. Compon. Packag. Manuf. Technol. **7** (2017) 964. https://doi.org/10.1109/TCPMT.2017.2694848
6 H. Chu, C. Jin, J. X. Chen, and Y. X. Guo: IEEE Trans. Antennas Propag. **63** (2015) 2375. https://doi.org/10.1109/TAP.2015.2411282
7 P. F. Hu, Y. M. Pan, X. Y. Zhang, and S. Y. Zheng: IEEE Trans. Antennas Propag. **65** (2017) 2079. https://doi.org/10.1109/TAP.2017.2670438
8 Y. Liu, S. H. Wang, N. Li, J. B. Wang, and J. P. Zhao: IEEE Antennas Wirel. Propag. Lett. **17** (2018) 1764. https://doi.org/10.1109/LAWP.2018.2864604
9 T. Le Nadan, J. P. Coupez, S. Toutain, and C. Person: Proc. 1998 28th European Microwave Conf. (IEEE, 1998) 672. https://doi.org/10.1109/EUMA.1998.338067
10 W. J. Wu, Y. Z. Yin, S. L. Shao, Z. Y. Zhang, and J. J. Xie: IEEE Antennas Wirel. Propag. Lett. **10** (2011) 1131. https://doi.org/10.1109/LAWP.2011.2171469
11 S. Y. Wang, F. Fan, Y. Li, S. W. Wong, R. Gomez-Garcia, L. Yang, and G. Zhang: IEEE Antennas Wirel. Propag. Lett. **20** (2021) 1626. https://doi.org/10.1109/LAWP.2021.3091999
12 Y. Yusuf, H. Cheng, and X. Gong: IEEE Trans. Antennas Propag. **59** (2011) 4016. https://doi.org/10.1109/TAP.2011.2164186
13 H. T. Cheng, Y. Yusuf, and X. Gong: IEEE Antennas Wirel. Propag. Lett. **10** (2011) 278. https://doi.org/10.1109/LAWP.2011.2135833
14 Q. Liu, L. Zhu, J. Wang, and W. Wu: IEEE Antennas Wirel. Propag. Lett. **19** (2020) 836. https://doi.org/10.1109/LAWP.2020.2981650
15 C. Z. Hua, M. Liu, and Y. L. Lu: Proc. Int. J. RF and Microwave Computer-Aided Engineering Conf. (2019) e21517. https://doi.org/10.1002/mmce.21517
16 T. Li and X. Gong: IEEE Trans. Microw. Theory Techn. **66** (2018) 3119. https://doi.org/10.1109/TMTT.2018.2832073
17 S. Ji, Y. Dong, Y. Pan, Y. L. Zhu, and Y. Fan: IEEE Trans. Antennas Propag. **69** (2020) 3155. https://doi.org/10.1109/TAP.2020.3037819
18 E. Y. Jung, J. W. Lee, T. K. Lee, and W. K. Lee: IEEE Trans. Antennas Propag. **60** (2012) 3632. https://doi.org/10.1109/TAP.2012.2201075
19 W. Zhan and Y. D. Dong: IEEE Access **7** (2019) 173007. https://doi.org/10.1109/ACCESS.2019.2956750
20 D. Deslandes and K. Wu: Proc. 2002 32nd European Microwave Conf. (IEEE, 2002) 1.https://doi.org/10.1109/EUMA.2002.339426
21 D. Deslandes and K. Wu: IEEE Trans. Microw. Theory Techn. **54** (2006) 2516. https://doi.org/10.1109/TMTT.2006.875807
22 Q. S. Wu, X. Zhang, and L. Zhu: IEEE Trans. Antennas Propag. **66** (2018) 5022. https://doi.org/10.1109/TAP.2018.2856104

About the Authors

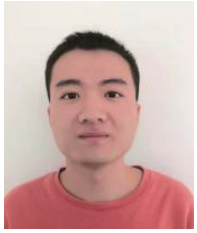

Jia-Xiang Chen was born in 1998 in Fujian Province, China. He received a bachelor's degree from Nanchang Hangkong University in 2020. He is currently working on his M.S. degree in information and communication engineering at Jimei University, Fujian Province, China. His research interest is in antenna techniques. (chenjx7335@jmu.edu.cn)

Hai-Tao Xing was born in 1983 in Shandong, China. In 2010, he obtained a master's degree in communication and information engineering from Ningbo University. At present, his main research interests are in embedded systems, artificial intelligence, and IoT. (xht2005@jmu.edu.cn)

You-Yi Ke was born in Fujian Province, China, in 1988. He received his B.S. degree from Jimei University in 2011. From 2011 to 2017, he was an RF engineer at Sanyuanda Communication Co., Ltd. Since 2017, he has been an R&D engineer at Ruijie Networks Co., Ltd. His research interests are in RF, WLAN, LTE, IoT, and other wireless networks. (kyy362615@163.com)

Chen Li was born in 1999 in Jiangsu Province, China. He received a bachelor's degree from Nanjing University of Posts and Telecommunications in 2020. He is currently working on his M.S. degree in information and communication engineering at Jimei University, Fujian Province, China. His research interest is in filter techniques. (li-chen321281@163.com)

Zhong-Hua Ma was born in Gansu, Republic of China, in 1973. He received his Ph.D. degree in microelectronics from Lanzhou University in 2018. His present research interests include antenna techniques, RF circuit design, RFID systems, and IoT. (mzhxm@jmu.edu.cn)